AGU PUBLICATIONS

Geophysical Research Letters

RESEARCH LETTER
10.1002/2015GL067228

Key Points:
- Midlevel highs over the Southern Hemisphere are an important component of summer climate
- Variability in these highs leads to large-scale drought/floods over the Southern Hemisphere
- Midlevel high and rainfall variability prominent on interannual and decadal scales

Correspondence to:
C. J. C. Reason,
Chris.Reason@uct.ac.za

Citation:
Reason, C. J. C. (2016), The Bolivian, Botswana, and Bilybara Highs and Southern Hemisphere drought/floods, *Geophys. Res. Lett.*, *43*, 1280–1286, doi:10.1002/2015GL067228.

Received 2 DEC 2015
Accepted 13 JAN 2016
Accepted article online 14 JAN 2016
Published online 4 FEB 2016

The Bolivian, Botswana, and Bilybara Highs and Southern Hemisphere drought/floods

C. J. C. Reason[1]

[1]Oceanography, University of Cape Town, Cape Town, South Africa

Abstract Semipermanent anticyclones in the midlevel troposphere over the subtropical landmasses are a prominent component of Southern Hemisphere climate. Typically, they occur over Bolivia, Botswana/Namibia, and northwestern Australia from austral spring to about April and are strongest in late summer. Here a mode of variability is studied that modulates the strength of these midlevel anticyclones and which is not strongly tied to El Niño–Southern Oscillation. This mode leads to variations in January–March rainfall over large parts of South America, southern Africa, and Australia on both interannual and near-decadal scales.

1. Introduction

During summer, semipermanent anticyclones occur over the subtropical landmasses in the Southern Hemisphere at midlevels (e.g., near 500 hPa). Although they are a prominent climatic feature, not much work has been done on these midlevel anticyclones. Their typical locations are over Bolivia in South America, Botswana/Namibia in southern Africa, and over Western Australia (WA); and they are understood to be thermally induced in response to heat released by tropical regions of high precipitation, located to their northeast. Thus, upper level divergence over the tropical high precipitation regions is mainly balanced by planetary vorticity advection implying equatorward flow to the south of the divergence maximum and high pressure to the west [*Lenters and Cook*, 1997]. The Bolivian High forms in response to heavy summer precipitation in the Amazon and the South Atlantic Convergence Zone (SACZ), whereas those over southern Africa and Australia lie roughly southwest of the high rainfall areas of the Congo and Indonesia, respectively. The Botswana High has not been much studied except regarding rainfall over Zimbabwe [*Matarira*, 1990; *Unganai and Mason*, 2002], and no studies seem to exist that focus on the high over WA.

Figure 1, National Centers for Environmental Prediction (NCEP) reanalysis mean 500 hPa geopotential height (GPH) field during late summer (January to March, JFM), shows a ridge of high pressure extending across the domain with closed anticyclones located over WA, Botswana/Namibia, the South Atlantic, and Bolivia. ERA shows similar results except that the Bolivian High is centered slightly further west. The relative low pressure between the Bolivian High and the South Atlantic ridge represents the SACZ. Although the Bolivian and Botswana Highs have been referred to as such in the literature, there appears to be no term for the corresponding feature in WA. Here it is referred to as the Bilybara High, the local Aboriginal word for "dry."

These midlevel anticyclones are most obvious in JFM. NCEP reanalyses [*Kalnay et al.,* 1996] suggest that they form at different times in spring. The Botswana High forms earliest with a closed anticyclone becoming evident in August, whereas the Bolivian and Bilybara Highs are first apparent in October. They then strengthen through spring and are strongly expressed over each landmass by December. January and February show the strongest anticyclones, while in March they weaken over each landmass and are no longer clearly evident in April. The Botswana High appears somewhat stronger in magnitude than the Bolivian or Bilybara Highs.

Figure 2 plots an index for each anticyclone (the standardized anomaly of JFM 500 hPa GPH averaged over the core region: 15–25°S, 60–70°W Bolivian High, 15–22°E Botswana High, and 115–125°E Bilybara High) showing variability in their intensity. The corresponding Bolivian, Botswana, and Bilybara Highs indices vary strongly in phase with each other (they correlate with each other at $r = 0.85$, significant at over 99%) with the strongest (weakest) highs evident during El Niño (La Niña) summers such as 1983, 1992, 1998, and 2010 (1989, 1996, 2000).

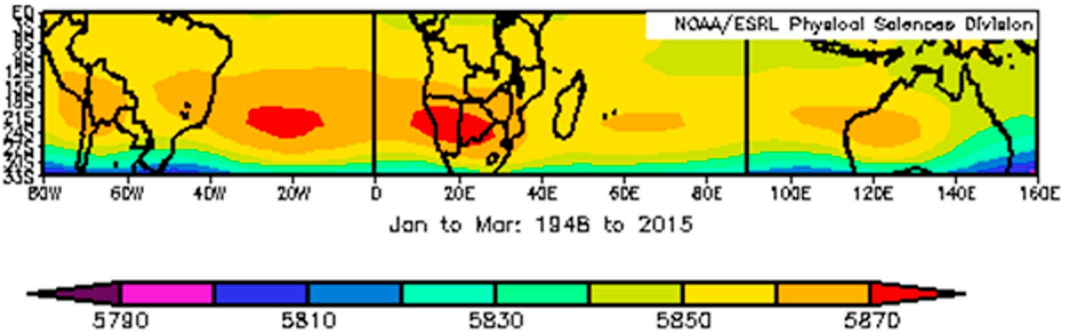

Figure 1. Climatological 500 hPa GPH for January to March (m).

While it seems obvious that El Niño–Southern Oscillation (ENSO) would impact these anticyclones, a mode of variability is considered here that appears to not be strongly related to ENSO and which modulates the strength of the Bolivian, Botswana and Bilybara Highs and hence summer rainfall over the three Southern Hemisphere landmasses.

2. Interannual Variability

Empirical orthogonal function (EOF) analysis of NCEP reanalysis 500 hPa GPH indicates that mode 2 has a pattern centered around the Botswana and Bilybara Highs and to some extent the Bolivian High (Figure 3a). Since the existence of these highs is related to tropical land-based precipitation, the domain for the EOF analysis was chosen to extend from just west of South America eastward to just east of Australia and from 10 to 33°S. Choosing the southern boundary as 33°S minimizes any influence from the Southern Annular Mode (SAM). ERA-Interim data give similar results, its time loading is correlated with the NCEP one at $r = 0.95$. This mode explains about 7% of the variance reflecting a pattern where the three highs vary in phase. Its associated time series Principal Component (PC2) (Figure 3b) is only weakly correlated with ENSO ($r = -0.19$ with Niño 3.4, significant at 90%), whereas the leading mode (78% of the variance) is strongly related to ENSO ($r = 0.84$, significant at 99.9%). Years with PC2 index values above 0.5 include five El Niños, five La Niñas, and five neutral summers; whereas when it is less than −0.5, there are four El Niños, five La Niñas, and six neutral summers. ENSO strongly influences summer rainfall over each landmass [*Allan et al.,* 1996; *Coelho et al*., 2002; *Lindesay*, 1988; *Reason et al*., 2000; *Tedeschi et al*., 2013]; however, the variability associated with mode 2 and its rainfall impacts has not been previously studied.

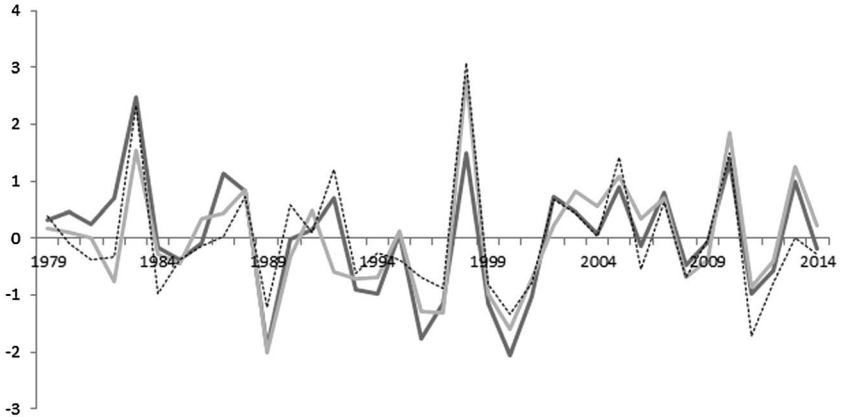

Figure 2. Indices for the Bolivian High (light grey), Botswana High (dark grey), and Bilybara High (black dotted) obtained from the standardized anomaly in 500 hPa GPH for JFM averaged over 60–70°W, 15–22°E, and 115–125°E, respectively, and 15–25°S in each case.

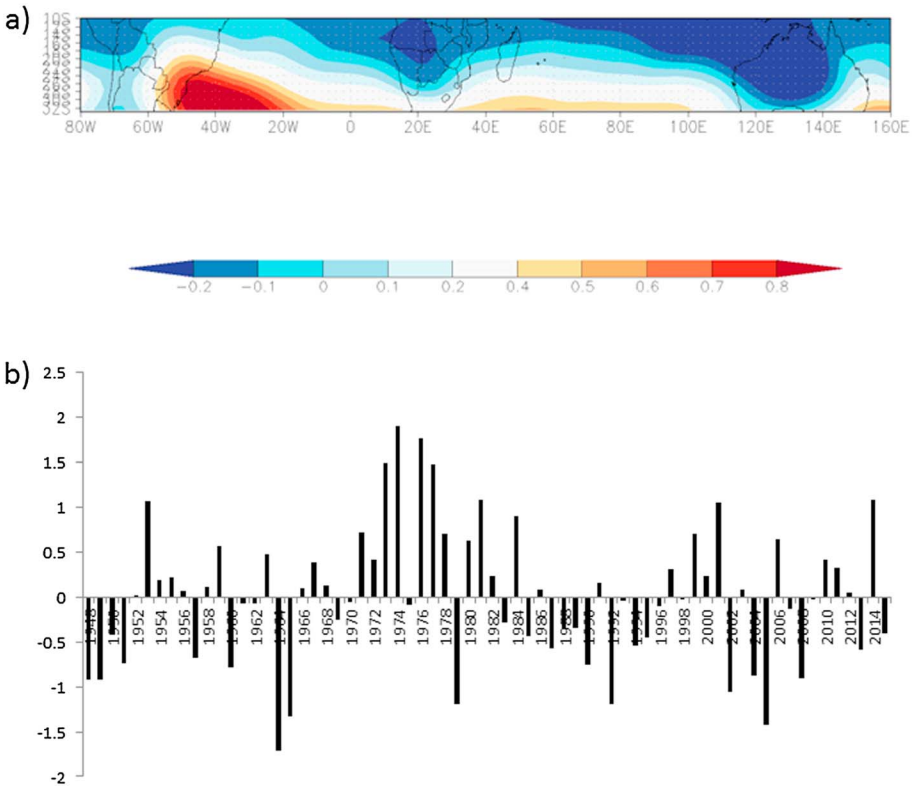

Figure 3. The second mode of 500 hPa GPH for JFM computed for the 80°W–160°E, 10–33°S sector of the Southern Hemisphere showing (a) EOF2 and its associated time series (b) PC2.

Figure 4 shows the strongest correlations between PC2 and sea surface temperature (SST) [*Smith and Reynolds*, 2004] in the southwest of each basin like those [*Fauchereau et al*., 2003; *Hermes and Reason*, 2005] found when correlating the South Indian Ocean subtropical dipole (SIOD) [*Behera and Yamagata*, 2001] with SST. The SIOD is only correlated with PC2 at $r = 0.36$ (95% significance) since the eastern SIOD pole lies much southward of Figure 4 negative correlation west of Sumatra. Only weak correlations exist with central Pacific SST. Figures 3, 4 are therefore consistent with a mode that is not strongly tied to ENSO. Nor is it strongly linked to the SAM (the correlation between the SAM index [*Marshall*, 2003] and PC2 is only 0.13). Composites of years with strong values of the PC2 index suggest that the SST variability (Figure 4) may be linked with changes in surface fluxes and Ekman heat transport [e.g., *Reason*, 1999].

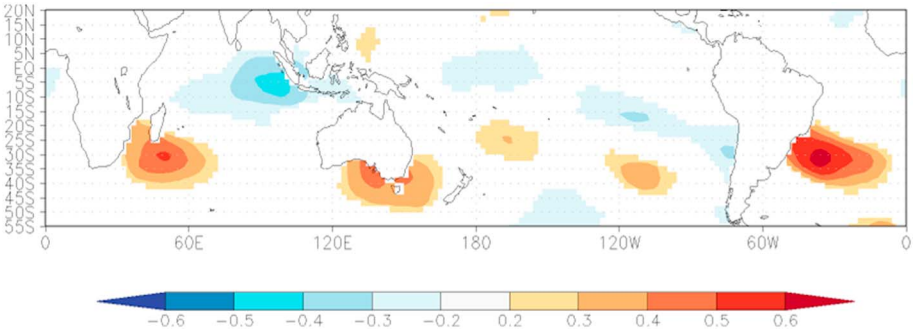

Figure 4. Correlation between PC2 and sea surface temperature for JFM—only grid boxes that are significant at 90% or more are plotted.

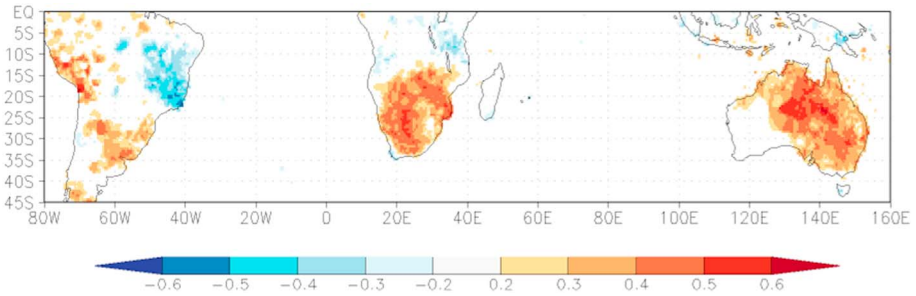

Figure 5. Correlation between PC2 and precipitation for JFM—only grid boxes that are significant at 90% or more are plotted.

Figure 5 correlates PC2 and summer precipitation using Global Precipitation Climatology Centre (GPCC) data [*Schneider et al*., 2008]. The patterns are stronger and spatially more extensive than when precipitation is correlated with Niño 3.4 or the Southern Oscillation Index (SOI). Large areas of southern Africa and the eastern two thirds of Australia are drier than average when the Botswana and Bilybara Highs are strong with enhanced subsidence through the troposphere over land. Over South America, the pattern is more complex due to the presence of the SACZ. Western and southeastern South America are dry when the Bolivian High is strong, whereas large areas of eastern Brazil are wet, reflecting a shift in the SACZ. The regions of positive correlation more or less match up with those showing negative correlation between PC2 and vertical velocity in the middle and upper tropospheres (Figure 6) reflecting stronger convection over the wetter areas when the Bolivian, Botswana, and Bilybara Highs are weak.

3. Decadal Variability

Figure 7 plots smoothed PC2 (using 7 year running means) as well as similarly smoothed spatially averaged JFM GPCC rainfall over South America (60–70°W, 12–23°S), southern Africa (16–38°E, 15–30°S), and Australia (135–155°E, 12–25°S). The resulting correlations between PC2 and the rainfall series are 0.72 (South America), 0.65 (southern Africa), and 0.72 (Australia), all 95% significant.

Figures 3 and 7 suggest substantial quasi-decadal variability in rainfall over the Southern Hemisphere landmasses associated with changes in these anticyclones. This variability seems most obvious during 1951–1998 after which it weakens and the time scale shortens. To illustrate its spatial extent and to remove any secular signal, Figure 8 plots epoch differences. Thus, Figure 8a indicates that 2002–2008 was anomalously dry over most of the areas of positive correlation (Figure 5) with stronger midlevel anticyclones compared to 1995–2001 which was anomalously wet with weaker anticyclones relative to 1985–1994 (Figure 8b) etc. Decadal rainfall variability has long been known over southern Africa [*Tyson et al*., 1975, 2002] and has been suggested as being related to regional SST [*Mason*, 1990; *Mason and Jury*, 1997],

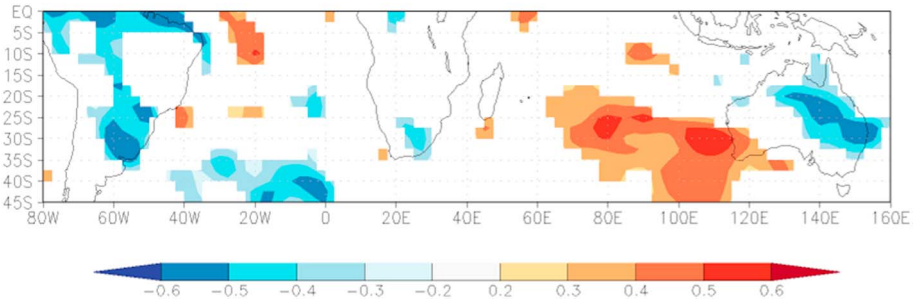

Figure 6. Correlation between PC2 and vertical velocity at 300 hPa for JFM—only grid boxes that are significant at 90% or more are plotted.

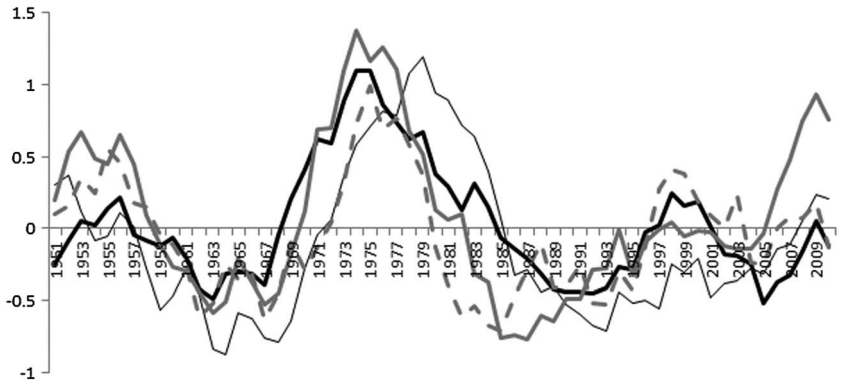

Figure 7. Smoothed (7 year running mean) time series of PC2 (black) and spatially averaged rainfall over South America (12–23°S, 60–70°W—fine black line), southern Africa (15–30°S, 16–38°E—dashed grey line), and eastern Australia (12–25°S, 135–155°E—dark grey line).

ENSO-like decadal patterns [*Reason and Rouault*, 2002], and variations in the SAM [*Malherbe et al*., 2014, 2015]. For Australia, the Interdecadal Pacific Oscillation, IPO [*Power et al*., 1999], variations in SAM [*Meneghini et al*., 2007] and regional anomalies in circulation and blocking [*Ansell et al*., 2000; *Smith et al*., 2000; *Risbey et al*., 2009] have been linked to decadal rainfall variability. Similarly, ENSO decadal variations have been linked with decadal rainfall variability in South America as have variations in Atlantic SST and its gradients [*Paegle and Mo*, 2002; *Marengo et al*., 2011; *Grimm and Saboia*, 2015]. It is beyond the scope here to determine the mechanisms behind the variability of Figures 7 and 8. However, it can be noted that only weak detrended correlations exist between PC2 (Figure 7) and a similarly smoothed SAM index [*Marshall*, 2003] ($r = 0.28$) or with IPO ($r = -0.32$) or with the Pacific Decadal Oscillation ($r = -0.09$).

The spatial extent of the rainfall differences is greatest over Australia. Over southern Africa, the epoch differences are also coherent and spatially extensive except in Figure 8a where the signal over northern Namibia is opposite to elsewhere between ~10°S and 34°S. For South America, northeastern Brazil tends to show opposite signals to that over Peru, southeastern South America, southern Africa, and eastern/northern Australia for almost all epochs, consistent with Figure 5. The epoch rainfall differences can be matched up with variations in middle and upper level vertical velocities and hence convection consistent with the changes in the Bolivian, Botswana, and Bilybara anticyclones.

Excepting the high rainfall areas in the Amazon and Congo and the Australian coast, the magnitudes of the differences are relatively large, about 50–300% of the JFM mean in many areas. This magnitude implies that there are may be substantial societal impacts in many areas associated with this variability in the anticyclones. Furthermore, this variability may have at times opposed the broad climate change signal of a generally wetter tropics and drier subtropics but reinforced it at other times during 1950–2014.

The larger magnitude of PC2 (Figure 7) in the 1970s is intriguing. Note that this is just before the introduction of satellite data into the reanalyses. However, the rainfall data, which have a substantial surface rain gauge component, also show large anomalies in this period. It is possible that these anomalies reflect the protracted La Niña episode (1974–1976) with very wet conditions over the Southern Hemisphere subtropics and hence are not unduly biased by the introduction of satellite data.

4. Summary

Little work has been done on the midlevel anticyclones that are prominent in summer over the Southern Hemisphere subtropics/tropics. The origin and relationship of the Bolivian High with South American precipitation has been studied [*Lenters and Cook*, 1997], whereas that over southern Africa (Botswana High) has only been briefly mentioned [*Matarira*, 1990; *Ratna et al*., 2012] and that over WA (Bilybara High) does not appear to have been examined. EOF analysis of 500 hPa GPH over the subtropics showed that the second

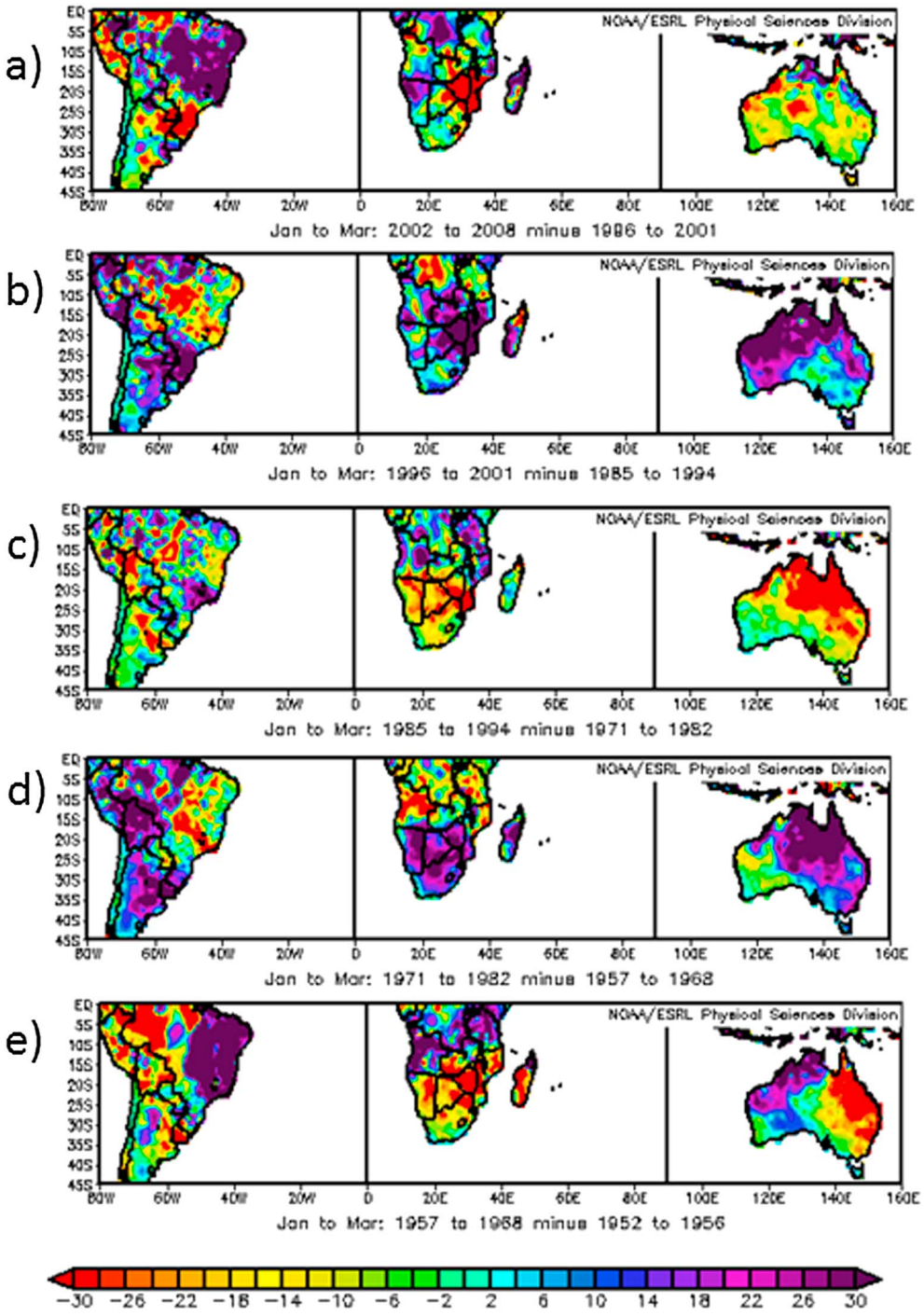

Figure 8. Epoch differences in JFM rainfall (mm/month).

mode, which is not strongly related to ENSO, involves an in-phase modulation of these three midlevel anticyclones which is linked to summer rainfall over large parts of Australia, southern Africa, and South America.

The relationship between this variability in the anticyclones and rainfall is expressed on both interannual and near-decadal time scales. For the latter, the relationship is strongest between about 1951 and 1998 after which it weakens and the time scale shortens. The magnitude of the associated rainfall variability is large relative to the mean implying that societal impacts of the quasi-decadal rainfall changes may be substantial.

Acknowledgments
NOAA (http://www.esrl.noaa.gov) and the KNMI (http://climexp.knmi.nl) are thanked for providing the freely accessible online data and plotting tools used in this study.

References

Allan, R. J., J. A. Lindesay, and D. E. Parker (1996), *El Niño–Southern Oscillation and Climatic Variability*, CSIRO, Collingwood, Victoria, Australia.
Ansell, T. J., C. J. C. Reason, I. N. Smith, and K. Keay (2000), Evidence for decadal variability in southern Australian rainfall and relationships with regional pressure and sea surface temperature, *Int. J. Climatol.*, *20*, 1113–1129.
Behera, S. K., and T. Yamagata (2001), Subtropical SST dipole events in the southern Indian Ocean, *Geophys. Res. Lett.*, *28*, 327–330.
Coelho, C. A. S., C. B. Uvo, and T. Ambrizzi (2002), Exploring the impacts of the tropical Pacific SST on the precipitation patterns over South America during ENSO periods, *Theor. Appl. Climatol.*, *71*, 185–197.
Fauchereau, N., S. Trzaska, Y. Richard, P. Roucou, and P. Camberlin (2003), Sea surface temperature co-variability in the Southern Atlantic and Indian Oceans and its connections with the atmospheric circulation in the southern hemisphere, *Int. J. Climatol.*, *23*, 663–677.
Grimm, A. M., and J. P. J. Saboia (2015), Interdecadal variability of the South American precipitation in the monsoon season, *J. Clim.*, *28*, 755–775.
Hermes, J. C., and C. J. C. Reason (2005), Ocean model diagnosis of interannual co-evolving SST variability in the South Indian and Atlantic Oceans, *J. Clim.*, *18*, 2864–2882.
Kalnay, E., et al. (1996), The NCEP/NCAR 40-year reanalysis project, *Bull. Am. Meteorol. Soc.*, *77*, 437–471.
Lenters, J. D., and K. H. Cook (1997), On the origin of the Bolivian high and related circulation features of the South American climate, *J. Atmos. Sci.*, *54*, 656–677.
Lindesay, J. A. (1988), South African rainfall, the Southern Oscillation and a Southern Hemisphere semi-annual cycle, *J. Clim.*, *8*, 17–30.
Malherbe, J., B. Dieppois, P. Maluleke, M. van Staden, and D. L. Pillay (2015), South African droughts and decadal variability, *Nat. Hazards*, doi:10.1007/s11069-015-1989-y.
Malherbe, J. A., W. A. Landman, and F. A. Engelbrecht (2014), The bi-decadal rainfall cycle, Southern Annular Mode and tropical cyclones over the Limpopo River basin, southern Africa, *Clim. Dyn.*, *42*, 3121–3138.
Marengo, J. A., J. Tomasella, L. M. Alves, W. R. Soares, and D. A. Rodriguez (2011), The drought of 2010 in the context of historical droughts in the Amazon region, *Geophys. Res. Lett.*, *38*, L12703, doi:10.1029/2011GL047436.
Marshall, G. J. (2003), Trends in the Southern Annular Mode from observations and reanalyses, *J. Clim.*, *16*, 4134–4143.
Mason, S. J. (1990), Temporal variability of sea surface temperature around southern Africa: A possible forcing mechanism for the eighteen-year rainfall oscillation?, *S. Afr. J. Sci.*, *86*, 243–252.
Mason, S. J., and M. R. Jury (1997), Climatic variability and change over southern Africa: A reflection on underlying processes, *Prog. Phys. Geogr.*, *21*, 23–50.
Matarira, C. H. (1990), Drought over Zimbabwe in a regional and global context, *Int. J. Climatol.*, *10*, 609–625.
Meneghini, B., I. Simmonds, and I. N. Smith (2007), Association between Australian rainfall and the Southern Annular Mode, *Int. J. Climatol.*, *27*, 109–121.
Paegle, J. N., and K. C. Mo (2002), Linkages between summer rainfall variability over South America and sea surface temperature anomalies, *J. Clim.*, *15*, 1389–1407.
Power, S., T. Casey, C. Folland, A. Colman, and V. Mehta (1999), Inter-decadal modulation of the impact of ENSO on Australia, *Clim. Dyn.*, *15*, 319–324.
Ratna, S. B., S. Behera, J. V. Ratnam, K. Takahashi, and T. Yamagata (2012), An index for tropical temperate troughs over southern Africa, *Clim. Dyn.*, *41*, 421–441.
Reason, C. J. C. (1999), Interannual warm and cool events in the subtropical/mid-latitude South Indian Ocean region, *Geophys. Res. Lett.*, *26*, 215–218, doi:10.1029/1998GL900285.
Reason, C. J. C., and M. Rouault (2002), ENSO-like decadal patterns and South African rainfall, *Geophys. Res. Lett.*, *29*(13), 1638, doi:10.1029/2002GL014663.
Reason, C. J. C., R. J. Allan, J. A. Lindesay, and T. J. Ansell (2000), ENSO and climatic signals across the Indian Ocean basin in the global context: Part I. Interannual composite patterns, *Int. J. Climatol.*, *20*, 1285–1327.
Risbey, J. S., M. J. Pook, P. C. McIntosh, M. C. Wheeler, and H. H. Hendon (2009), On the remote drivers of rainfall variability in Australia, *Mon. Weather Rev.*, *137*, 3233–3253.
Schneider, U., T. Fuchs, A. Meyer-Christoffer, and B. Rudolf (2008), Global precipitation analysis products of the GPCC. Global Precipitation Climatology Centre (GPCC), Deutscher Wetterdienst. [Available online at ftp://ftp-anon.dwd.de/pub/data/gpcc/PDF/GPCC_intro_products_2008.pdf.]
Smith, I. N., P. McIntosh, T. J. Ansell, C. J. C. Reason, and K. L. McInnes (2000), South-west Western Australian winter rainfall and its association with Indian Ocean climate variability, *Int. J. Climatol.*, *20*, 1913–1930.
Smith, T. M., and R. W. Reynolds (2004), Improved extended reconstruction of SST (1854–1997), *J. Clim.*, *17*, 2466–2477.
Tedeschi, R. G., I. F. A. Cavalcanti, and A. M. Grimm (2013), Influences of two types of ENSO on South American precipitation, *Int. J. Climatol.*, *33*, 1382–1400.
Tyson, P. D., T. G. J. Dyer, and M. N. Mametse (1975), Secular changes in South African rainfall: 1880 to 1972, *Q. J. R. Meteorol. Soc.*, *101*, 817–833.
Tyson, P. D., G. R. J. Cooper, and T. S. McCarthy (2002), Millenial to multidecadal variability in the climate of southern Africa, *Int. J. Climatol.*, *22*, 1105–1117.
Unganai, L., and S. Mason (2002), Long-range predictability of Zimbabwe summer rainfall, *Int. J. Climatol.*, *22*, 1091–1103.